
Research Article: New Research | Development

Neuregulin-4 is required for maintaining soma size of pyramidal neurons in the motor cortex

<https://doi.org/10.1523/ENEURO.0288-20.2021>

Cite as: eNeuro 2021; 10.1523/ENEURO.0288-20.2021

Received: 2 July 2020

Revised: 5 January 2021

Accepted: 8 January 2021

This Early Release article has been peer-reviewed and accepted, but has not been through the composition and copyediting processes. The final version may differ slightly in style or formatting and will contain links to any extended data.

Alerts: Sign up at www.eneuro.org/alerts to receive customized email alerts when the fully formatted version of this article is published.

Copyright © 2021 Paramo et al.

This is an open-access article distributed under the terms of the Creative Commons Attribution 4.0 International license, which permits unrestricted use, distribution and reproduction in any medium provided that the original work is properly attributed.

1 **Neuregulin-4 is required for maintaining soma size of pyramidal neurons**
2 **in the motor cortex**

3
4 **Abbreviated title:** Nrg4 and pyramidal neuronal soma size

5
6
7 Blanca Paramo, Sven O. Bachmann, Stéphane J. Baudouin,
8 Isabel Martinez-Garay and Alun M. Davies

9
10 School of Biosciences, Cardiff University, Museum Avenue, Cardiff CF10 3AX, Wales

11
12 **Author contribution:** BP, SOB and SJB performed the research; BP analysed the data; BP,
13 IM-G and AMD designed the research; BP and AMD wrote the paper. AMD and IM-G
14 supervised the research.

15 **Correspondence:** Blanca Paramo. School of Biosciences, Cardiff University, Museum
16 Avenue, Cardiff CF10 3AX, Wales. Email: ParamoB@cardiff.ac.uk

17 **Number of figures:** 7 Figures

18 **Number of words for Abstract:** 232

19 **Number of words for Significance Statement:** 88

20 **Number of words for Introduction:** 431

21 **Number of words for Discussion:** 1572

22 **Acknowledgements:** This work was supported Wellcome Trust grant 103852 to AMD. BP
23 was supported by CONACyT fellowship number 740520.

24 **Conflict of interest:** Authors report no conflict of interest.

25 **Funding sources:** This work was supported by the Wellcome Trust Grant Number 103852 to
26 AMD. BP was supported by a fellowship from CONACyT number 740520.

27
28
29

30 **Abstract**

31 The regulation of neuronal soma size is essential for appropriate brain circuit function
32 and its dysregulation is associated with several neurodevelopmental disorders. A defect in the
33 dendritic growth and elaboration of motor neocortical pyramidal neurons in neonates lacking
34 neuregulin-4 (NRG4) has previously been reported. In this study, we investigated if the loss
35 of NRG4 causes further morphological defects that are specific to these neurons. We
36 analysed the soma size of pyramidal neurons of layers 2/3 and 5 of the motor cortex and a
37 subpopulation of multipolar interneurons in this neocortical region in *Nrg4*^{+/+} and *Nrg4*^{-/-}
38 mice. There were significant decreases in pyramidal neuron soma size in *Nrg4*^{-/-} mice
39 compared with *Nrg4*^{+/+} littermates at all stages studied (P10, P30 and P60). The reduction
40 was especially marked at P10 and in layer 5 pyramidal neurons. Soma size was not
41 significantly different for multipolar interneurons at any age. This *in vivo* phenotype was
42 replicated in pyramidal neurons cultured from *Nrg4*^{-/-} mice and was rescued by neuregulin-4
43 treatment. Analysis of a public single-cell RNA sequencing repository revealed discrete *Nrg4*
44 and *Erb4* expression in subpopulations of layer 5 pyramidal neurons, suggesting that the
45 observed defects were due in part to loss of autocrine Nrg4/Erb4 signalling. The pyramidal
46 phenotype in the motor cortex of *Nrg4*^{-/-} mice was associated with a lack of Rotarod test
47 improvement in P60 mice, suggesting that absence of NRG4 causes alterations in motor
48 performance.

49
50

51 **Significance Statement**

52 Neuregulins are growth factors that are abundantly expressed in the nervous system
53 where they regulate a plethora of processes essential for normal nervous system development
54 and function in adulthood. Dysregulation of neuregulin signalling has been implicated in
55 neurodevelopmental disorders, thus characterising the particular functions of members of this
56 family of proteins is highly relevant for understanding how such disorders emerge. This study
57 shows that neuregulin-4 is required to maintain motor cortex pyramidal neuron soma size,
58 and that altered pyramidal neuronal morphology is associated with motor defects in mice.
59

60 **Introduction**

61

62

63 Neuregulins are signalling proteins that are abundantly expressed in the nervous
64 system where they are required for neuronal development and brain function. Since the
65 discovery of the first member of this family of proteins (NRG1), 5 other members have been
66 described, each one with multiple isoforms generated by alternative splicing (Aono et al.,
67 2000; Kanemoto et al., 2001; Hayes and Gullik, 2008). Neuregulins bind and activate
68 members of the ErbB family of receptor tyrosine kinases which regulate many aspects of cell
69 function including survival, differentiation, growth and proliferation (Falls 2003). In the
70 nervous system, neuregulin (NRG1) is involved in the development of neurons and glial cells
71 (Cespedes et al., 2018), NRG2 and NRG3 have roles in synaptogenesis and synaptic function,
72 while NRG5 and NRG6, although less extensively studied, are highly expressed in the brain
73 where NRG6 is required for radial migration in the neocortex (Mei and Nave, 2014; Zhang et
74 al., 2013). In contrast, the role of NRG4 in the developing brain has only recently been
75 studied. Neocortical pyramidal neurons and striatal medium spiny neurons from mice lacking
76 NRG4 exhibit shorter and less elaborated dendrites (Paramo et al., 2018, 2019).

76

77 Neurons acquire a polarized morphology while they migrate to cortical layers,
78 establish connections and form functional circuits. Failure to acquire and maintain an
79 adequate size, appropriately extend and elaborate processes and form functional synapses
80 results in impaired neuronal function and is associated with neurodevelopmental disorders
81 (Parenti et al., 2020). The alterations in dendritic growth and elaboration in neocortical
82 pyramidal neurons lacking NRG4 that have previously been reported led us to explore
83 whether these neurons display further morphological defects caused by the loss of
84 NRG4/ErbB4 signalling. We analysed the cell body size of layer 2/3 (L2/3) and layer 5 (L5)
85 neocortical pyramidal neurons as well as a subpopulation of interneurons (multipolar) in the
86 motor cortex of *Nrg4*^{-/-} and *Nrg4*^{+/+} mouse brains. Layer 5 pyramidal neurons were the most
87 affected by the loss of NRG4, exhibiting a <20% reduction in soma size at P10. In contrast,
88 the overall morphology of multipolar cortical interneurons was not altered, including the cell
89 body size and dendritic length and complexity. This defect was replicated in cultured cortical
90 pyramidal neurons, and was restored to normal by treatment with NRG4 protein in young
91 developing neurons. These morphological defects were associated with deficiencies in motor
92 functions in NRG4-null mice as assessed by Rotarod performance. Overall, our results
93 suggest that NRG4 plays an important role in the acquisition and maintenance of the
appropriate morphology of a subset of neurons in the motor cortex and in motor function.

94

95 **Materials and methods**

96

97 *Animals*

98 All animal procedures were performed in accordance with [Authors University]
99 animal care committee's regulation. Mice were housed in a 12h light-dark cycle with access
100 to food and water *ad libitum*. Mice lacking functional *Nrg4* expression caused by retroviral
101 insertion of a gene trap between exons 1 and 2 were obtained from the Mutant Mouse
102 Resource Centre, UC Davies (California, USA). Mice were backcrossed from a C57BL/6
103 background into a CD1 background. *Nrg4*^{+/+} and *Nrg4*^{-/-} mice were generated by crossing
104 *Nrg4*^{+/+}. Male and female mice were separated after weaning (3-4 weeks after birth) and kept
105 with littermates (4-5 mice per cage). For the behavioural assays, postnatal day 60 (P60) mice
106 were handled for 2 days before the test. The behavioural tests were performed during the
107 light cycle.

108

109 *Immunohistochemistry*

110 Wildtype postnatal P10 and P30 mice were perfused and post-fixed for 16 and 3 hrs,
111 respectively, in 4% paraformaldehyde in 0.12 M phosphate-buffered saline (PBS) at 4C.
112 After fixation, brains were washed 3 times with PBS and sectioned using a vibratome. 50 µm
113 sections were collected in multi-well plates, permeabilised in 0.1% Triton in PBS, heated in
114 10 mM sodium citrate buffer for 5 min at 95C, washed and blocked in 5% BSA, 3% donkey
115 serum, 0.1% Triton serum in PBS (blocking solution) for 1 h at RT and incubated with
116 primary antibodies in 5x diluted blocking solution as follows: anti-Nrg4 (1:100, abcam anti-
117 rabbit polyclonal antibody ab19247) anti-Nrg4 (20 µg/ml, abcam anti-mouse monoclonal
118 antibody ab239580), anti-ErbB4 (5 µg/ml, abcam anti-mouse monoclonal antibody ab19391),
119 anti-Fezfz (1:500, abcam anti-rabbit polyclonal antibody ab69436), anti-Gpr88 (10 µg/ml,
120 Novus Biologicals anti-rabbit polyclonal antibody NBP1-02330) overnight at 4C. Unbound
121 primary antibody was washed 3 times with PBS and slices were incubated with fluorophore-
122 conjugated secondary antibodies (1:500, Donkey anti-rabbit, rat or mouse Alexa-488 and
123 Alexa-594) for 1 h at RT. Slices were then washed 3 times with PBS, incubated in DAPI
124 (1:4000) for 15 min and mounted on microscope slides using DAKO mounting medium.
125 Sections were visualized using a Zeiss LSM 780 confocal microscope and ZEN Black
126 software (version 2.0).

127

128 *Analysis of neuronal soma size*

129 Golgi-Cox impregnation was performed on 150 μm coronal sections of P10, P30 and
130 P60 $Nrg4^{+/+}$ and $Nrg4^{-/-}$ mouse brains by the FD Rapid GolgiStain kit (FD
131 Neurotechnologies) according to manufacturer's instructions. Pyramidal neuronal soma size
132 (area and perimeter) were quantified in micrographs using FIJI (Image J) by tracing the
133 outline of neuronal somata. The soma area and perimeter of a total of 90 pyramidal neurons
134 per genotype at each age ($n = 30$ neurons per mouse, $n = 3$ mice per genotype at each age) of
135 layers 2/3 and layer 5 of the motor cortex was measured and analysed. Regarding
136 interneurons, due to the heterogeneity of interneuronal morphology, three different types of
137 interneurons were clearly identified in Golgi preparations: basket, bipolar and multipolar
138 interneurons, the latter being the most abundant. Therefore, we quantified the soma and
139 perimeter of multipolar interneurons in the same way as for pyramidal neurons and, in
140 addition, we measured dendritic complexity using the Neurite tracer plug of FIJI, and the
141 Sholl profile of reconstructed neurons, as previously described (Paramo et al., 2018). The
142 soma area, perimeter and dendritic complexity of a total of 30 of multipolar interneurons per
143 genotype at each age ($n = 10$ neurons per mouse, $n = 3$ mice per genotype at each age) were
144 analysed.

145 For the *in vitro* analysis of neuronal soma size, pyramidal neurons from E16 $Nrg4^{+/+}$
146 and $Nrg4^{-/-}$ cortices were cultured as previously described (Paramo et al., 2018). After 3 days
147 *in vitro* (DIV), neurons were fluorescently labelled with calcein-AM (2 $\mu\text{g}/\text{ml}$) for 15 min at
148 37C. For the 9 DIV experiments, neurons were transfected after 7 days *in vitro* with a GFP
149 plasmid (1 $\mu\text{g}/\text{ml}$) using lipofectamine for 3h. 2 days later, neurons were fixed using 4%
150 paraformaldehyde, washed and kept in PBS. In some experiments, CD1 or $Nrg4^{-/-}$ neurons
151 were treated with 100 or 1000 ng/ml recombinant NRG4 (Thermo Fisher Scientific).
152 Micrographs of fluorescently labelled neurons at 3 and 9 DIV were taken using an Axiovert
153 200 Zeiss fluorescent microscope. The soma area of cultured pyramidal neurons was
154 quantified using FIJI (Image J) as described for the Golgi images. A total of 90 neurons per
155 age per condition from three independently generated cortical cultures were analysed.

156

157 *Rotarod tests*

158 Male $Nrg4^{+/+}$ and $Nrg4^{-/-}$ mice were tested for motor defects using the Rotarod. On the
159 day of the experiment, mice were placed on a rod that accelerated to 40 rpm within 5

160 minutes. The latency to fall was measured across seven subsequent trials and is expressed as
161 the time spent on the rod until the test mouse fell off, gripped to the rod, followed the rod for
162 a full rotation or the test ended after 5 min. The performance of each individual was also
163 compared by obtaining the slope (b) values of each curve after logarithmic regression
164 ($y = b \log x + a$).

165

166 *Elevated plus maze test*

167 Male and female *Nrg4*^{+/+} and *Nrg4*^{-/-} mice were tested for changes in levels of anxiety
168 using the elevated plus maze assay. On the day of the test, each mouse was placed at the
169 centre of the maze and recorded for 5 mins. A tracking software (EthoVision XT, Noldus)
170 was used to quantify the time spent in the open arms as more anxious mice spend less time
171 there. The sum of the time spent in the left plus right open arms was calculated and
172 compared.

173

174 *Open-field test*

175 In addition to the elevated plus maze, anxiety was evaluated in adult male and female
176 *Nrg4*^{+/+} and *Nrg4*^{-/-} mice using the open field test. On the day of the test, each mouse was
177 placed at the centre of an open-field arena (40 x 40 cm) in the dark and recorded for 20 min.
178 The total distance travelled and the time spent in the centre of the arena were automatically
179 obtained by the tracking software EthoVision.

180

181 *Novel object recognition test*

182 Changes in the ability of mice to react to novelty were evaluated using the novel
183 object recognition test. Adult male and female *Nrg4*^{+/+} and *Nrg4*^{-/-} mice were placed in an
184 open-field containing 2 equal objects attached to the floor (familiarization) and recorded for 5
185 min. The next day, mice were placed in the open-field containing a familiar object and a
186 novel object and were recorded for 5 min (test). The time spent exploring either object was
187 automatically obtained by the tracking software EthoVision. The time spent exploring either
188 object on the familiarization day (same object) and on the test day (familiar and novel object)
189 were plotted for comparison. To calculate the percentage of object discrimination, the time
190 spent exploring the novel object was divided by the total time spent exploring multiple by
191 100.

192

193 *Statistical analysis*

194 Data were analysed using GraphPad Prism 8 and are expressed as mean \pm standard
195 error of mean (SEM). For analysis of *in vivo* soma size, values were compared by one-way
196 ANOVA with Fisher's *post hoc* test for multiple comparisons. *In vitro* differences in soma
197 size and rescue by recombinant NRG4 were analysed by one-way ANOVA with Tukey's
198 *post hoc* test for multiple comparison. For the Rota rod test, data were compared by repeated
199 measures ANOVA followed by Bonferroni *post hoc* test for multiple comparison.
200 Logarithmic regression of all individual mice performance was performed to obtain slope or
201 b values from the equation $y = b \log x + a$. b values were then compared by an unpaired one-
202 tailed *t* test (increase latency as increased performance). Novel object recognition data from
203 *Nrg4*^{+/+} mice were compared after normalization by a *t* test. Adjusted *p* values were
204 considered significant as follows: *****p*<0.0001, ****p*<0.001, ***p*<0.01 and **p*<0.05.
205

206 Results

207

208 ***Nrg4* and *ErbB4* mRNAs are expressed in discrete populations of cortical neurons of the** 209 **anterolateral motor cortex**

210 Neuregulin 4 expression in different brain regions of the developing mouse brain has
211 been recently reported (Paramo et al., 2018), while the expression of its receptor ErbB4 has
212 long been known to be high in cortical interneurons (Mei and Nave, 2014). A shortcoming of
213 the former study is that estimation of NRG4 mRNA levels in different brain regions does not
214 reveal which kinds of cells express NRG4 in these regions. However, single-cell public RNA
215 sequencing repositories, where the transcriptome of different subclasses of cells is established
216 and the expression of particular genes can be obtained and analysed, can be used to determine
217 which kinds of cells express different levels of particular genes. We used the public
218 repository published by Tasic and colleagues in 2018 where the authors analysed cell types in
219 the adult mouse anterior lateral motor cortex (ALM) and the primary visual cortex (VISp)
220 (Tasic et al., 2018). Tasic and colleagues established 4 classes of cortical cells: glutamatergic,
221 GABAergic, non-neuronal and endothelial cells. Glutamatergic and GABAergic classes were
222 further divided in subclasses and clusters based on the presence of specific markers or the
223 localisation of those neurons. *Nrg4* mRNA was expressed across all classes in a 4.5%
224 fraction in glutamatergic neurons, 3.2% in GABAergic neurons, and 0.57% and 0.29% in
225 non-neuronal and endothelial cells, respectively (Fig 1A). In contrast and as previously
226 reported, *ErbB4* mRNA was mostly expressed in GABAergic neurons (80.7%), and to a
227 lesser extent in glutamatergic (3.2%), non-neuronal (6.2%) and endothelial (0.59%) cells.
228 Based on the previously reported observation that the loss of NRG4 specifically affects the
229 morphology of pyramidal neurons, we selected the ‘glutamatergic class’ to determine the
230 proportion of neurons in all its subclasses expressing *Nrg4* mRNA and *ErbB4* mRNA. *Nrg4*
231 mRNA was expressed in all the glutamatergic subclasses in the following fraction: layer 2/3
232 **7.2%**, layer 4 **5.7%**, layer 5 IT (intratelencephalic) **4.08%**, layer 6 IT **4.9%**, layer 5 PT
233 (pyramidal tract) **4.17%**, NP (near-projecting) **1.99%**, L6 CT (corticothalamic) **3.2%** and
234 layer 6b **2.78%**, while *ErbB4* mRNA was only expressed in >1% of all the glutamatergic
235 subclasses in layer 5 IT neurons (**9.2%**, Fig. 1B). Since the glutamatergic subclass with the
236 highest fraction of neurons expressing both the ligand and the receptor mRNAs was the layer
237 5 IT subclass, we decided to further analyse the levels of *Nrg4* mRNA and *ErbB4* mRNA in
238 each cluster from the ‘ALM layer 5 IT’ subclass. We found similar levels of *Nrg4* mRNA
239 and *ErbB4* mRNA in the majority of neurons in the following 6 out of the 9 clusters that

240 comprise this subclass (% *Nrg4* mRNA; % *ErbB4* mRNA): layer 5 IT *Pld5* (15 and 7%), layer
241 5 IT *Cbln4 Fezf2* (17 and 7%), layer 5 IT *Lypld1 Gpr88* (14 and 16%), layer 5 IT *Tnc* (20
242 and 55%), layer 5 IT *Tmem163 Dmrtb1* (21 and 19%), L5 IT *Tmem163 Arhgap25* (31 and
243 9%, Fig. 1C).

244

245 *Nrg4* and *ErbB4* are co-expressed with FEZF2 and GPR88 in layer 5 cortical neurons of the
246 motor cortex during development

247 The above results suggest that *Nrg4* and *ErbB4* are at least partially co-expressed in the same
248 type of neurons. To verify these data, we conducted immunolabeling experiments e used
249 FEZF2, a transcription factor previously reported to be involved in dendritic arborisation and
250 the development of spines of layer 5 pyramidal neurons (Chen et. al., 2005) and GPR88 a G-
251 protein-coupled receptor that is expressed in the cortex to regulate multisensory integration, a
252 function of the cortex altered in neuropsychiatric disorders (Ehrlich et al., 2018). We
253 conducted double immune-labelling in the motor cortex of P10 and P30 wildtype mice. We
254 observed co-expression of NRG4 with FEZF2 and GPR88 in the deep layers of the motor
255 cortex at P10 and P30, although the levels of FEZF2 seemed to be lower at P30 (Fig. 1-D-F
256 and L-N). To further support these findings, we used CTIP2, a developmental transcription
257 factor, and the major downstream FEZF2 effector (Chen et. al., 2008). In the motor cortex of
258 wildtype mice at P10, we observed co-expression of FEZF2 and CTIP2, as expected, but
259 more importantly of CTIP2 and NRG4 and CTIP2 and ERBB4, although few cells with no
260 co-expression were also observed (Fig 7). Furthermore, we also observed co-localisation of
261 ERBB4 and the two markers tested above, FEZF2 and GPR88 at P10 and P30 (Fig. 1G-I and
262 O-Q). Lastly, we also observed co-expression of NRG4 and ERBB4 in the motor cortex at
263 P10 and P30 (Fig.1 J-K and R-S). Taken together, these observations corroborate the single-
264 cell RNA sequencing data, and show that *Nrg4* contributes to pyramidal neuronal
265 development. These results from our IHC experiments strengthen and extend the conclusion
266 about the contribution of NRG4 to developing pyramidal neurons that is likely to be mediated
267 either partly or entirely by an autocrine mechanism, although from the lack of co-expression
268 in a proportion of neurons we can not rule out the participation of a paracrine mechanism.

269

270 **Absence of NRG4 causes a decrease in soma size of pyramidal neocortical neurons *in***
271 ***vivo***

272 It has been previously reported that the loss of NRG4 impairs the development of
273 dendrites, reducing the size and complexity of the dendritic tree of pyramidal neurons of the

274 motor cortex (Paramo et al., 2018). To further investigate the morphological effects caused
275 by the loss of NRG4 expression in neocortical pyramidal neurons, we examined cell size of
276 pyramidal neurons in layers 2/3 and 5 in *Nrg4*^{-/-} and *Nrg4*^{+/+} mice at two postnatal ages (P10
277 and P30) and in adults (P60). Golgi preparations of coronal sections from the most rostral
278 part of the neocortex, including the frontal/motor cortex and the most rostral region of the
279 somatosensory cortex were used to measure soma size (area and perimeter) of pyramidal
280 neurons. In layer 2/3, we found similar significant reductions in both soma size and perimeter
281 in *Nrg4*^{-/-} mice compared with *Nrg4*^{+/+} littermates at P10 (area $p = 0.0105$; perimeter $p =$
282 0.0305), P30 (area $p = 0.0267$; perimeter $p = 0.0123$) and P60 (area $p = 0.0079$; perimeter $p =$
283 0.0040) (Fig. 2A-C). The average reductions in pyramidal neuron soma area in *Nrg4*^{-/-} mice
284 were 8.5%, 8.8% and 4% in P10, P30 and P60 mice, respectively. In layer 5, we also
285 observed significant reductions in pyramidal neuron soma area and perimeter in *Nrg4*^{-/-} mice
286 compared with *Nrg4*^{+/+} littermates at all stages studied: P10 (area $p < 0.0001$; perimeter
287 $p < 0.0001$), P30 (area $p = 0.0115$; perimeter $p = 0.0123$) and P60 (area $p = 0.0344$; perimeter
288 $p = 0.0404$) (Fig. 2D-F). However, the reductions at P10 were quantitatively greater and more
289 highly significant than at later ages. At P10 there was a 22% reduction in the soma area of
290 layer 5 pyramidal neurons in *Nrg4*^{-/-} mice compared with *Nrg4*^{+/+} littermates.

291

292 **Absence of NRG4 does not significantly affect soma size of neocortical multipolar** 293 **interneurons *in vivo***

294 To determine if the effect of NRG4 deficiency on soma size was pyramidal neuron
295 specific or if it affected other neuronal types in the neocortex, we evaluated the soma size of
296 a population of interneurons. Bipolar, basket and multipolar interneurons (Ascoli et al., 2008)
297 were evident in our Golgi preparations, but because multipolar interneurons were the most
298 abundant we focused our analysis on these neurons. In addition to assessing soma size (area
299 and perimeter), we also quantified the size and complexity of their dendritic arbors (total
300 dendrite length, total number of branch points and Sholl profiles). We did not find any
301 significant differences in cell body size (Fig. 3A-C, H-J). The area and perimeter of *Nrg4*^{+/+}
302 interneurons were (mean \pm SEM) $201.2 \pm 9.6 \mu\text{m}^2$ and $58.73 \pm 1.4 \mu\text{m}^2$, respectively, while
303 *Nrg4*^{-/-} area and perimeter were (mean \pm SEM) $214.8 \pm 11.13 \mu\text{m}^2$ and $58.08 \pm 1.48 \mu\text{m}^2$ (Fig.
304 3B, C). At P10 the total dendritic length was (mean \pm SEM) $323.2 \pm 17 \mu\text{m}^2$ and $326.6 \pm$
305 $12.46 \mu\text{m}^2$ for *Nrg4*^{+/+} and *Nrg4*^{-/-}, respectively (Fig. 3D), while the number of branching
306 points was (mean \pm SEM) 3.7 ± 0.26 for *Nrg4*^{+/+} and 4.2 ± 0.24 for *Nrg4*^{-/-} (Fig. 3E). The

307 total number of dendrites was also similar (mean \pm SEM) 9.9 ± 0.35 in *Nrg4*^{+/+} multipolar
308 interneurons and 10.5 ± 0.38 in *Nrg4*^{-/-} (Fig. 3F). The lack of differences was reflected in the
309 almost completely overlapping Sholl profiles (Fig. 3G). At P30, A small but non-significant
310 ($p = 0.1988$) difference was observed in the total soma area between genotypes (mean \pm
311 SEM: $254.6 \pm 10.25 \mu\text{m}^2$ vs $235.4 \pm 10.63 \mu\text{m}^2$; Fig. 3I). The dendritic outgrowth was similar
312 among genotypes (Fig. 3K-N). Taken together, the above findings suggest that NRG4 plays
313 an important role in promoting and maintaining soma size of pyramidal neurons in the
314 developing neocortex, especially those of layer 5, without significantly affecting the size and
315 dendritic morphology of multipolar interneurons.

316

317 **Neocortical pyramidal neurons cultured from *Nrg4*^{-/-} mice replicate the small soma** 318 **phenotype**

319 To determine if the small soma phenotype observed *in vivo* in *Nrg4*^{-/-} pyramidal
320 neocortical neurons is exhibited by pyramidal neurons cultured from *Nrg4*^{-/-} mice and to
321 ascertain if this defect can be rescued by recombinant NRG4 treatment, we established
322 cortical cultures from E16 *Nrg4*^{+/+} and *Nrg4*^{-/-} embryos. Pyramidal soma size (area and
323 perimeter) was assessed after 3 and 9 days. This analysis was facilitated by labelling the cells
324 with either calcein-AM after 3 days in culture or by GFP transfection after 7 days in culture
325 for analysis at 9 days *in vitro*. After 3 and 9 DIV, soma area and perimeter were significantly
326 smaller in cultures established from *Nrg4*^{-/-} embryos compared with those established from
327 *Nrg4*^{+/+} embryos (Fig. 4). At 3 DIV, a 13.3% reduction in soma area in *Nrg4*^{-/-} ($p < 0.0001$)
328 and a 6.3% reduction in perimeter ($p = 0.0003$) of pyramidal neurons was observed and it
329 was significantly rescued by recombinant NRG4 (100 ng/ml) (area $p = 0.0002$; perimeter $p =$
330 0.0011 ; Fig. 4A-C). No significant differences were observed in the soma area (mean \pm SEM:
331 $167.6 \pm 4.04 \mu\text{m}^2$ vs $164.6 \pm 2.94 \mu\text{m}^2$, respectively; adjusted p value 0.8106) or in the
332 perimeter (mean \pm SEM: $49.93 \pm 0.6 \mu\text{m}^2$ vs $49.65 \pm 0.51 \mu\text{m}^2$, respectively, adjusted p value
333 0.9343,) between *Nrg4*^{+/+} and *Nrg4*^{-/-}+NRG4 neurons, which indicates full rescue by NRG4.

334 At 9 DIV, the soma of *Nrg4*^{-/-} pyramidal neurons was 21.6% smaller (area $p < 0.0001$;
335 perimeter $p < 0.0001$), and significantly rescue by NRG4 (area $p = 0.0090$; perimeter
336 $p = 0.0069$). However, NRG4 did not fully rescue the reduction in soma area and perimeter in
337 this case, since *Nrg4*^{+/+} vs *Nrg4*^{-/-}+NRG4 values were still significantly different (mean area
338 \pm SEM: $258.3 \pm 8.3 \mu\text{m}^2$ vs $233.1 \pm 6.49 \mu\text{m}^2$, respectively; adjusted p value 0.0384; mean
339 perimeter \pm SEM: $64.25 \pm 1.31 \mu\text{m}^2$ vs $60.62 \pm 0.98 \mu\text{m}^2$, respectively; adjusted p value

340 0.0378).

341 These results show that the small soma pyramidal neuron phenotype observed *in vivo*
342 in NRG4-deficient mice is replicated in cultured neurons and is fully rescued in young
343 developing neurons and partially rescued in more mature neurons by soluble NRG4.

344

345 **Defects in motor performance of mice lacking *Nrg4***

346 The morphological defects observed in motor cortex pyramidal neurons led us to
347 evaluate whether these alterations have an impact on the ability of mice to execute a motor
348 task, such as the rotarod test. We evaluated P60 *Nrg4*^{+/+} and *Nrg4*^{-/-} mice performance,
349 measured as the time spent on the rod over time (7 trials, T1-T7). *Nrg4*^{+/+} performance
350 improved with subsequent trials and the latency at T6 was significantly different when
351 compared to T1 (latency (mean ± SEM) at T1 = 131.4 ± 27.9 s versus latency at T6 = 283.7 ±
352 12.4 s, $p = 0.0078$; Fig. 5A). However, *Nrg4*^{-/-} mice did not improve their performance
353 (latency (mean ± SEM) at T1 = 167.5 ± 21.1 s versus 220.5 ± 29.5 s at T6 and 209.5 ± 32.9 s
354 at T7; Fig. 3A). The average slope values from each individual animal tested acquired after
355 logarithmic regression from *Nrg4*^{+/+} and *Nrg4*^{-/-} were significantly different ($p = 0.0425$;
356 Fig.5B). Individual traces of T1 and T7 from all the animals tested are shown in Fig. 3C.
357 These results suggest that the morphological defects in pyramidal neocortical motor cortex
358 neurons caused by the loss of *NRG4* impact the motor ability of mice.

359

360 **No differences in anxiety levels or response to novelty**

361 The defects observed in the morphology of pyramidal neurons of the motor cortex
362 caused a defect in motor skills in adult mice. We also evaluated if the lack of NRG4 affected
363 other behaviour. We evaluated anxiety levels using the elevated plus maze and open-field test
364 as well as the response to novelty using the novel object recognition test between genotypes.
365 Adult (P60) *Nrg4*^{-/-} mice spent slightly less time in the open arms of the maze but this
366 decrease was not significant (Fig. 6A). No differences were observed in the distance travelled
367 (Fig. 6B) or in the time spent in the centre of the open-field (Fig. 6C). When exposed to a
368 novel object, the *Nrg4*-null mice spent a similar amount of time (mean ± SEM) exploring the
369 familiar (116.6 ± 17.61 s) and novel object (119.7 ± 17.53 s); while *Nrg4*^{+/+} mice spent more
370 time exploring the novel (119.4 ± 19.06 s) than the familiar object (79.77 ± 10.86 s), but this
371 difference was not significantly different (Fig. 6D). However, this increase was significantly
372 different ($p = 0.0462$) when the data from *Nrg4*^{+/+} mice were normalized to the time spent
373 exploring the familiar object in the familiarization day, and then compared by an unpaired t

374 test (mean \pm SEM) 0.95 ± 0.14 for the familiar object on test day vs 1.96 ± 0.54 for the novel
375 object on the test day. These observations were reflected in the object discrimination
376 percentage, where the percentage in *Nrg4*^{+/+} vs *Nrg4*^{-/-} mice was slightly reduced from 58.15
377 ± 6.5 % to 50.6 ± 6.6 %, but no significantly different ($p = 0.4366$; Fig. 6E).
378

379 **Discussion**

380 Neuregulins play a diverse and critical role in the development of the nervous system.
381 NRG4 function in the developing motor cortex contributes to the dendritic outgrowth and
382 complexity of pyramidal neurons. However, further morphological defects in pyramidal
383 neurons or other type of cortical neurons lacking NRG4 have not been investigated and the
384 functional consequences of such defects have not been studied. Neuronal morphological
385 defects greatly impact the function of the circuits, causing neurodevelopment disorders. Thus,
386 defining the morphological defects caused by altered NRG4/ErbB4 signalling and their
387 functional consequences aids in our understanding of the crucial mechanisms required for
388 normal cortical development and function in the adulthood. In addition, the identification of
389 more specifically affected populations of neurons allows the development of targeted
390 interventions to prevent these defects. In this study, we analysed the cell soma of neocortical
391 pyramidal and multipolar interneurons of *Nrg4*^{+/+} and *Nrg4*^{-/-} mice motor cortex at different
392 stages to identify whether the loss of NRG4 affects soma size, and whether this effect was
393 general or specific to certain populations of neurons. We found an important decrease in the
394 soma size of L2/3 and more significantly of L5 pyramidal neurons with no changes in the
395 size of multipolar interneurons or layer 6 pyramidal neurons (not shown) lacking NRG4.
396 Data obtained from a single-cell RNA-sequencing public repository, show that *Nrg4* and
397 *ErbB4* mRNAs were mostly co-expressed in glutamatergic L5 neurons of the adult anterior
398 lateral motor cortex suggesting that a cell-autonomous NRG4/ErbB4 function is required to
399 maintain the soma size of L5 pyramidal neurons. Furthermore, and to validate these
400 observations, double immuno-labelling of pyramidal neurons from the motor cortex showed
401 that NRG4 and ErbB4 are co-expressed with markers that define specific subpopulations of
402 excitatory neurons of the anterolateral motor cortex, such as *Fezf2* and *Grp88*. At P10 *Fezf2*
403 and *Gpr88* were found to be co-expressed with both ErbB4 and NRG4. To further strengthen
404 these observations, we also found co-expression with the *Fezf2*-downstream effector *Ctip2*
405 for both NRG4 and ErbB4, although neurons with no co-expression of both markers were
406 also found. At P30, the number of *Fezf2*-positive neurons decreased, but *Gpr88* was still
407 found to be co-expressed with ErbB4 and NRG4. In addition, ErbB4 and NRG4 were also
408 found to be co-expressed in layer 5 motor cortex pyramidal neurons. The observation that
409 only a proportion of neurons co-expressed both markers and the ligand or receptor suggests
410 that a paracrine mechanism can not be ruled out.

411 The mechanisms controlling cell body size in post-mitotic neurons function
412 differently than in dividing cells since in the later these pathways also regulate cell cycle

413 progression and division. However, the observation that this effect is also observed *in vitro*
414 suggests that NRG4 may be acting in a cell-autonomous manner to regulate neuronal soma
415 size by modulating an intrinsic mechanism. To date, none of the neuregulins nor ErbB4 itself
416 has been reported to control neuronal soma size in the CNS. NRG1 cystein-rich domain
417 isoform, the most abundant isoform in the brain, is required to maintain an
418 excitatory/inhibitory balance between interneurons and pyramidal cells (Agarwal et al.,
419 2014), whereas NRG2, expressed at P7 in the hippocampus and neocortex, localizes to the
420 soma and dendrites of hippocampal neurons (Longart et al., 2004), where it downregulates
421 glutamatergic transmission by promoting the internalization of GluN2B-containing NMDA
422 receptors (Vullhorst et al., 2015). Deletion of *ErbB4* in neocortical excitatory neurons alters
423 dendritic spine maturation (Cooper and Koleske 2014). However, these studies did not look
424 at the effects of neuregulin deletion or overexpression on overall neuronal morphology nor in
425 the potential role of neuregulins in the acquisition and maintenance of neuronal size. In
426 mouse models of genetic disorders that result in dendritic abnormalities such as Rett
427 syndrome, a decrease in the soma size of hippocampal neurons was observed (Rangasamy et
428 al., 2016), while loss of function mutations in the tuberous sclerosis complex (TSC), a
429 negative regulator of the mTOR/Akt pathway, increase the soma size of hippocampal
430 pyramidal neurons but decrease the density of dendritic spines causing alterations in
431 glutamatergic transmission (Tavazoie et al., 2005). Likewise, depleted c-Jun N-terminal
432 kinase 1 signal increases L5 motor cortex pyramidal neuron dendritic length and increases
433 soma size (Komulainen et al., 2014). The decrease in dendritic architecture observed in *Nrg4*
434 knockout pyramidal neocortical neurons is consistent with a decrease in soma size, since
435 there is a correlation between dendritic and cell body size (van Pelt et al., 1996).
436 Furthermore, the lack of differences between soma size and dendritic complexity in a
437 subpopulation of interneurons in *Nrg4* knockout mice supports this observation. The
438 possibility of alterations in the morphology of other types of interneurons remains, since
439 multipolar interneurons are only a fraction of this diverse class of neurons. In our analysis,
440 the multipolar interneurons we measured are biochemically defined by calbindin expression.
441 This population of interneurons is also transcriptomically defined by parvalbumin and
442 somatostatin expression, according to the clusters described in the single-cell RNA
443 sequencing study. All the interneurons in this cluster express *ErbB4* and in fact, *NRG3* is
444 expressed in 56%, *NRG2* in 17%, while *NRG1* and *NRG4* are expressed only in 4.5 and 3.5%
445 of these interneurons, respectively. The levels of NRG3 and NRG2 in these interneurons with
446 high ErbB4 expression may explain why the signalling can be maintained in these neurons

447 and thus why the size of the soma is not affected. The more significant decrease in soma size
448 we observed, that is, in layer 5 pyramidal neurons, correlated with the levels of *Nrg4* and
449 *ErbB4* mRNA co-expression. Layer 5 intratelencephalic pyramidal neurons project axons
450 within the telencephalon. In contrast to cortical sensory areas, layer 5 pyramidal neurons in
451 the anterolateral motor cortex display slower dynamics and are involved in controlling
452 movement planning, among other functions (Svoboda and Li 2018). Consistent with the
453 phenotypical defects observed in *Nrg4* knockout neurons, the clusters with similar levels of
454 receptor and ligand co-expression are defined by markers related to cytoskeletal dynamics,
455 synaptic function, dendritic arborization and spine formation, migration and axonal
456 development, and have been reported to be altered in neurodevelopmental disorders. For
457 example, *Fezf2* is a transcription repressor that is implicated in the development of dendritic
458 arborization and spines of large layer 5 pyramidal neurons (Chen et al., 2005) a population of
459 neurons affected in schizophrenia (Shepherd 2013). Interestingly, *ErbB4* has been reported to
460 be a susceptibility gene for this disease (Silberberg et al., 2006). In addition, *Gpr88* encodes a
461 G-protein-coupled receptor that is expressed in the cortex to regulate multisensory
462 integration, a function of the cortex altered in neuropsychiatric disorders (Ehrlich et al.,
463 2018). Lastly, *Arhgap25* encodes a Rho GTPase activating protein (GAP), that acts as a
464 negative regulator of Rho GTPases, proteins implicated in actin remodelling, cell polarity and
465 migration (Hodge and Ridley 2016). GAP activity is required to regulate Rac1 activation
466 since alterations in this pathway have been implicated in intellectual disability (Lelieveld et
467 al., 2016), a neurodevelopmental disorder characterised by defects in network connectivity
468 and unbalanced excitation and inhibition in the cerebral cortex.

469 Importantly, the morphological defects caused by the loss of NRG4 caused an
470 impairment in the motor skills of adult mice, while total motor activity, anxiety and response
471 to novelty were unaffected. This can be in part due to the fact that the brain areas mediating
472 these behaviours are unaffected in *Nrg4* knockout mice, or maybe other neuregulins can
473 compensate for the loss of NRG4 in specific areas where these neuregulins are more
474 abundant. In agreement with our observation, genetic models where the function of
475 downstream effectors of ErbB4 signalling such as Akt and mTOR is inhibited in a brain-
476 specific manner or by rapamycin treatment display impair rotarod performance (Thomanetz
477 et al., 2013; Bergeron et al., 2014). Importantly, together with the requirement of NRG4 for
478 maintaining soma size, the defects observed in overall dendritic outgrowth are likely to be a
479 major contributor of the defects in performing the rotarod task. Although we cannot
480 completely rule out a contribution from the cerebellum in the motor defects observed in the

481 *Nrg4*-null mice, we have found that at P12, Purkinje neurons from *Nrg4* knockout mouse
482 brains did not display any significant morphological defects (data not shown). However,
483 morphological or any other physiological alterations in other cell types that comprise the
484 cerebellum cannot be discarded as contributors to the motor phenotype. We therefore cannot
485 attribute the motor deficiencies to the morphological defects observed in the motor cortex
486 without considering that alterations in the cerebellum can also be accounted for these
487 deficiencies in performing a motor task.

488 Further studies where NRG4 is specifically deleted in pyramidal neurons will inform
489 more as to the requirement of NRG4/ErbB4 signalling for circuit formation and function.
490 Likewise, the generation of transgenic lines where *Nrg4* is depleted specifically in other
491 populations of CNS neurons may be informative.

492 Taken together, our observations indicate that NRG4 plays a broader biological role
493 in the control of neuronal morphology. Our results show that NRG4 is important for the
494 development and maintenance of the morphology of neocortical pyramidal neurons of the
495 motor cortex, and that some populations rely more on its expression early during
496 development to acquire normal size. Besides its role in development, its expression in motor
497 areas in the adult mouse brain in transcriptomically defined populations of pyramidal neurons
498 shows that it may be required for the specific adequate function of these neurons and perhaps
499 its loss or altered expression, which in turns would affect NRG4/ErbB4 signalling, may
500 contribute to the pathogenesis of neurodevelopmental or psychiatric disorders.

501 **References**

502

503 Aono S, Keino H, Ono T, Yasuda Y, Yoshihito T, Matsui F, Taniguchi M, Sonta S, Oohira A
504 (2000) Genomic organization and expression pattern of mouse neuroglycan C in the
505 cerebellar development. *J Biol Chem* 275:337- 342.

506

507 Ascoli G, Alonso-Nanclares L, Anderson S. *et al.* (2008) Petilla terminology: nomenclature
508 of features of GABAergic interneurons of the cerebral cortex. *Nat Rev Neurosci* 9:557–568.

509

510 Bergeron Y, Chagniel L, Bureau G, Massicotte G, Cyr M (2014) mTOR signaling contributes
511 to motor skill learning in mice. *Front Mol Neurosci* 7:26.

512

513 Cespedes JC, Liu M, Harbuzariu A, Nti A, Onyekaba J, Cespedes HW, Bharti PK, Solomon
514 W, Anyaoha P, Krishna S, Adjei A, Botchway F, Ford B, Stiles JK (2018) Neuregulin in
515 Health and Disease. *Int J Brain Disord Treat* 4:024.

516

517 Chen JG, Rasin MR, Kwan KY, Sestan N, (2005) Zfp312 is required for subcortical axonal
518 projections and dendritic morphology of deep-layer pyramidal neurons of the cerebral
519 cortex. *Proc Natl Acad Sci* 102:17792–17797.

520

521 Chen B, Wang SS, Hattox AM, Rayburn H, Nelson SB, McConnell SK (2005)
522 The *Fezf2–Ctip2* genetic pathway regulates the fate choice of subcortical projection
523 neurons in the developing cerebral cortex. *PNAS* 105:11382-11387.

524

525 Cooper, MA, Koleske AJ (2014) Ablation of ErbB4 from excitatory neurons leads to reduced
526 dendritic spine density in mouse prefrontal cortex. *J Comp Neurol* 522:3351-3362.

527

528 Ehrlich AT, Semache M, Bailly J, Wojcik S, Arefin TM, Colley C, Le Gouill C, Gross F,
529 Lukashева V, Hogue M, Darcq E, Harsan LA, Bouvier M and Kieffer BL (2018) Mapping
530 GPR88-Venus illuminates a novel role for GPR88 in sensory processing. *Brain Struct*
531 *Funct* 223:1275–1296.

532

533 Falls DL (2003) Neuregulins: functions, forms, and signalling strategies. *Experimental Cell*
534 *Research* 284:14-30.

535

- 536 Hayes NVL, Gullick WJ (2008) The Neuregulin Family of Genes and their Multiple Splice
537 Variants in Breast Cancer. *J Mammary Gland Biol Neoplasia* 13:205.
538
- 539 Hodge RG and Ridley AJ (2016) Regulating Rho GTPases and their regulators. *Nature Rev*
540 *Moll Cell Biol* 17:496-510.
541
- 542 Jones PL and Jones FS (2000) Tenascin-C in development and disease: gene regulation and
543 cell function. *Matrix Biol* 19:581-96.
544
- 545 Irintchev A, Rollenhagen A, Troncoso E, Kiss JE, Schachner M (2005) Structural and
546 Functional Aberrations in the Cerebral Cortex of Tenascin-C Deficient Mice. *Cerebral*
547 *Cortex* 15: 950–962.
548
- 549 Kanemoto, N, Horie M, Omori K, Nishino N, Kondo M, Noguchi, K, Tanigami A (2001)
550 Expression of TMEFF1 mRNA in the mouse central nervous system: precise examination
551 and comparative studies of TMEFF1 and TMEFF2. *Mol Brain Res* 86:48-55.
552
- 553 Lelieveld S, Reijnders M, Pfundt R. et al., (2016) Meta-analysis of 2,104 trios provides
554 support for 10 new genes for intellectual disability. *Nat Neurosci* 19:1194–1196.
555
- 556 Longart M, Liu Y, Karavanova I and Buonanno A (2004) Neuregulin-2 is developmentally
557 regulated and targeted to dendrites of central neurons. *J Comp Neurol* 472:156-172.
558
- 559 Mei L, Nave KA (2014) Neuregulin-ERBB signaling in the nervous system and
560 neuropsychiatric diseases. *Neuron* 83:27-49.
561
- 562 Paramo B, Wyatt S and Davies AM (2018) An essential role for neuregulin in the growth and
563 elaboration of developing neocortical pyramidal dendrites. *Exp Neurol* 302:85-92.
564
- 565 Paramo B, Wyatt S and Davies AM (2019) Neuregulin-4 is required for the growth and
566 elaboration of striatal medium spiny neuron dendrites. *J Neuropathol Exp Neurol* 78:725-34.
567

- 568 Parenti I, Rabaneda LG, Schoen H and Novarino G (2020) Neurodevelopmental disorders:
569 From genetics to functional pathways. *Trends in Neurosciences*. In Press
570 doi.org/10.1016/j.tins.2020.02.004
571
- 572 Rangasamy S, Olfers S, Gerald B, Hilbert A, Svejda S and Narayanan V (2016) Reduced
573 neuronal size and mTOR pathway activity in the Mecp2 A140V Rett syndrome mouse
574 model. *Fl1000Research* 5:2269.
575
- 576 Sekeljic V and Andjus PR (2012) Tenascin-C and its functions in neuronal plasticity. *Int J*
577 *Biochem Cell Biol* 44:825-9.
578
- 579 Shepherd GM (2013) Corticostriatal connectivity and its role in disease. *Nat Rev Neurosci*
580 14, 278–291.
581
- 582 Silberberg G, Darvasi A, Pinkas-Kramarski R, Navon R (2006) The involvement of ErbB4
583 with schizophrenia: association and expression studies. *Am J Med Genet B Neuropsychiatr*
584 *Genet* 141:142-148.
585
- 586 Tasic, B, Yao, Z., Graybuck LT, et al., (2018) Shared and distinct transcriptomic cell types
587 across neocortical areas. *Nature* 563:72–78.
588
- 589 Tavazoie SF, Alvarez VA, Ridenour DA, Kwiatkowski DJ and Sabatini BL (2005)
590 Regulation of neuronal morphology and function by the tumor suppressors Tsc1 and Tsc2.
591 *Nature Neuroscience* 8:1727-1734.
592
- 593 Thomanetz V, Angliker N, Cloetta D, Lustenberger RM, Schweighauser M, Oliveri F, Suzuki
594 N, Ruegg MA (2013) Ablation of the mTORC2 component rictor in brain or Purkinje cells
595 affects size and neuron morphology. *Journal of Cell Biology* 201:293-308.
596
- 597 van Pelt J, Van Ooyen A, and Corner MA (1996) Growth cone dynamics and activity-
598 dependent processes in neuronal network development. *Prog Brain Res* 108:333–346.
599

600 Vullhorst D, Mitchell R, Keating C, Roychowdhury S, Karavanova I, Tao-Cheng JH and
601 Buonanno A (2015) A negative feedback loop controls NMDA receptor function in cortical
602 interneurons via neuregulin 2/ErbB4 signalling. *Nat Commun* 6:7222.

603

604 Zhang C, Mejia LA, Huang ., Valnegri P, Bennett EJ, Anckar J, Jahani-Asl A, Gallardo G,
605 Ikeuchi Y, Yamada T, Rudnicki M, Harper JW, Bonni A, (2013) The X-linked intellectual
606 disability protein PHF6 associates with the PAF1 complex and regulates neuronal migration
607 in the mammalian brain. *Neuron* 78:986-993.

608

609 **Figure legends**

610

611 **Figure 1. *Nrg4* and *ErbB4* mRNA expression in single cells of the adult mouse cortex**
612 **obtained from RNA-sequencing public repository data. (A)** Fraction in percentage of
613 single cells expressing *Nrg4* (purple) and *ErbB4* (violet) in each class of cells: Glutamatergic,
614 GABAergic, Non-neuronal and Endothelial. **(B)** Fraction and levels of expression of *Nrg4*
615 and *ErbB4* mRNA in 7 subclasses of glutamatergic cortical neurons. **(C)** *Nrg4* and *ErbB4*
616 mRNA levels of expression in single cells in all the clusters in the glutamatergic neurons
617 class from the anterior lateral motor cortex layer 5 intratelencephalic (L5 IT ALM) subclass.
618 Postnatal day 10 **(D-I)** and 30 **(L-Q)** immunohistochemical co-labelling of NRG4 and *Fezf2*,
619 NRG4 and *Gpr88*, *ErbB4* and *Fezf2*, *ErbB4* and *Gpr88*. **(R-S)** NRG4 and *ErbB4* co-
620 expression at P10 and P30. Arrows indicate co-expression of both proteins. Dashed boxes
621 indicate where higher magnifications were taken from. Scale bar high magnification 100 μm
622 and 50 μm lower magnification.

623

624 **Figure 2. Neuronal soma size is decreased in motor cortex L2/3 and L5 neocortical**
625 **pyramidal neurons of *Nrg4*^{-/-} mice.** Representative micrographs of Golgi-impregnated
626 pyramidal neurons in L2/3 **(A)** and L5 **(D)** of the motor cortex at P10, P30 and P60 *Nrg4*^{+/+}
627 and *Nrg4*^{-/-} mice. Scale bar = 25 μm . **(B, E)** Quantification of the area and perimeter **(C, F)**.
628 One-way ANOVA with Fisher's post hoc test for multiple comparison, ****p<0.0001,
629 ***p<0.001, **p<0.01, * p<0.05.

630

631 **Figure 3. Unaffected neuronal morphology and soma size of multipolar interneurons**
632 **from *Nrg4*^{-/-} mice. (A, H)** Representative micrographs of Golgi-stained multipolar
633 interneurons from *Nrg4*^{+/+} and *Nrg4*^{-/-} mice at P10 and P30, respectively. Scale bar = 25 μm .
634 Total area **(B, I)**, perimeter **(C, J)**, total dendritic length **(D, K)**, number of branch points **(E,**
635 **L)**, number of dendrites **(F, M)** and Sholl analysis **(G, N)**.

636

637 **Figure 4. Neuronal soma size is reduced *in vitro* in *Nrg4*^{-/-} pyramidal neurons and it is**
638 **rescued by NRG4 treatment. (A)** Representative micrographs of cortical pyramidal neurons
639 from *Nrg4*^{+/+} and *Nrg4*^{-/-} embryos at 3 and 9 DIV stained with calcein-AM (upper panel), and
640 transfected with GFP (lower panel), respectively. *Nrg4*^{-/-} neurons were treated with
641 recombinant NRG4 (100 ng/ml). Scale bar =20 μm . Quantification of the area **(B and D)** and

642 perimeter (C and E) of 90 neurons per condition. One-way ANOVA with Tukey's *post hoc*
643 test for multiple comparison, **** $p < 0.0001$, *** $p < 0.001$ ** $p < 0.01$.

644

645 **Figure 5. The loss of NRG4 impairs motor skills.** (A) *Nrg4*^{+/+} P60 male mice spent
646 significantly more time on the accelerating rotarod after trial 6 compared to *Nrg4*^{-/-} mice.
647 Data are mean ± SEM. Repeated measurements ANOVA with Bonferroni's multiple
648 comparison test vs T1. ** $p < 0.01$ (B) Comparison of slope values from each animal tested
649 obtained after logarithmic regression of each individual performance. Unpaired t-test
650 * $p < 0.05$. (C) Traces of individual performance (T1 to T7).

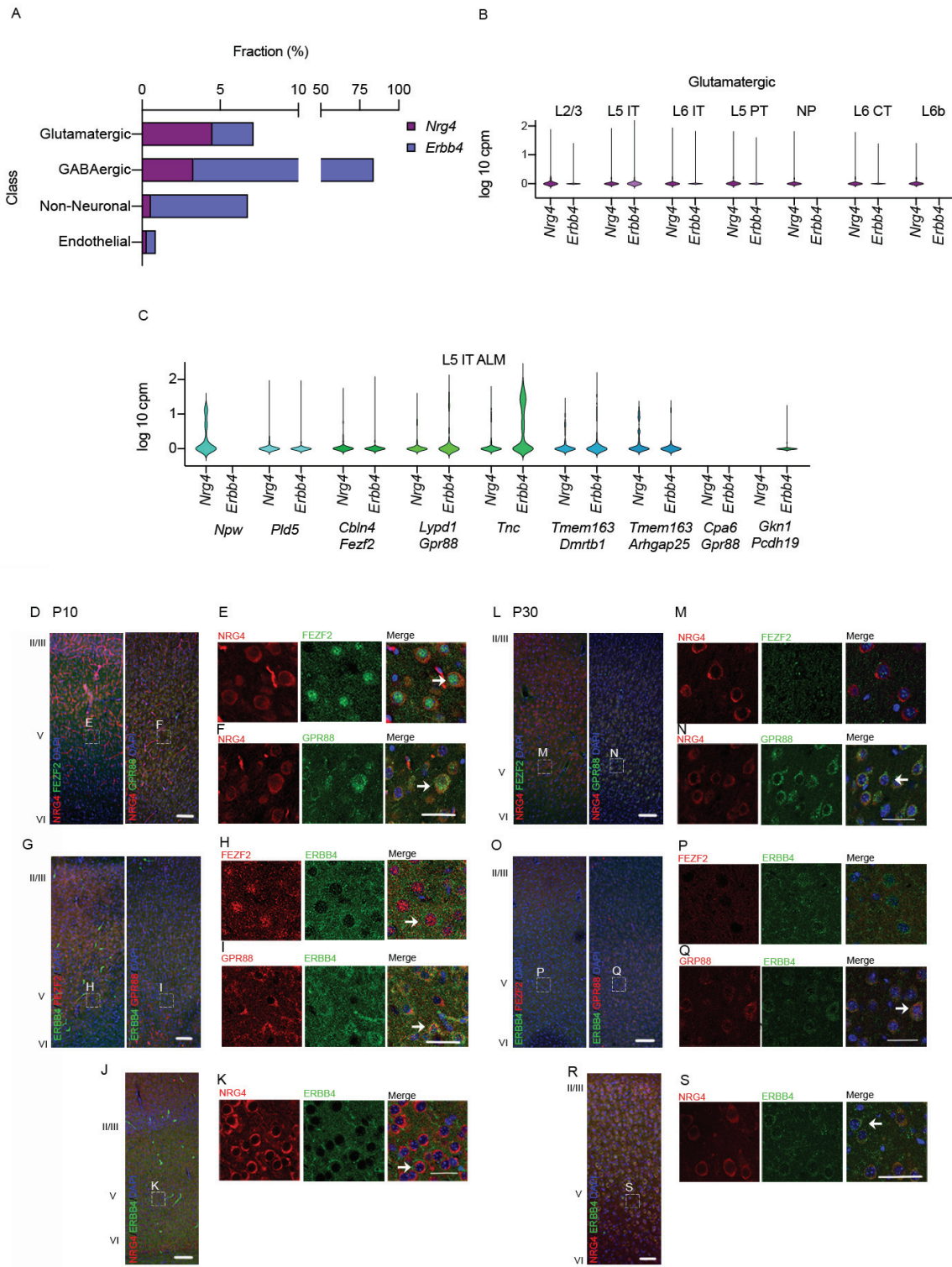
651

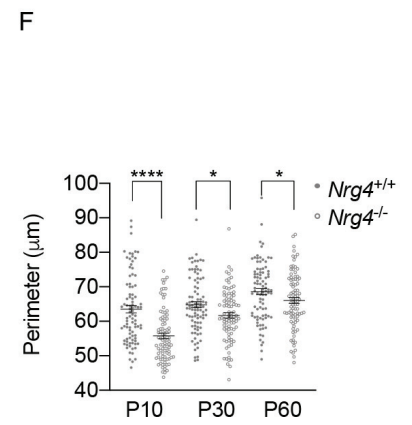
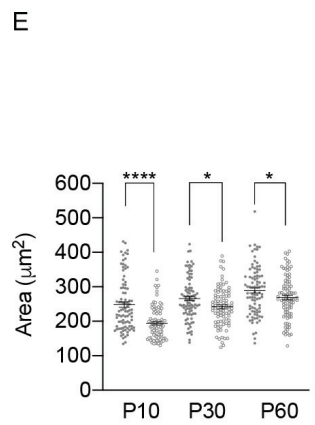
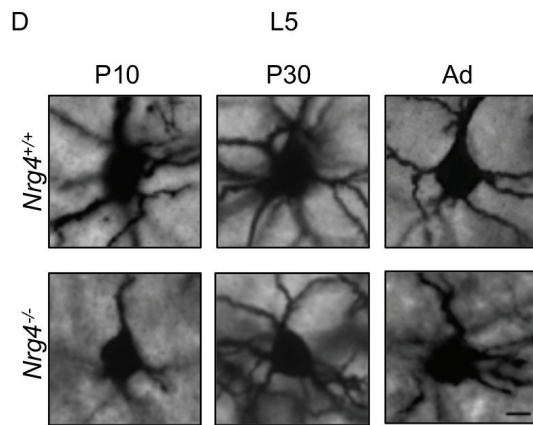
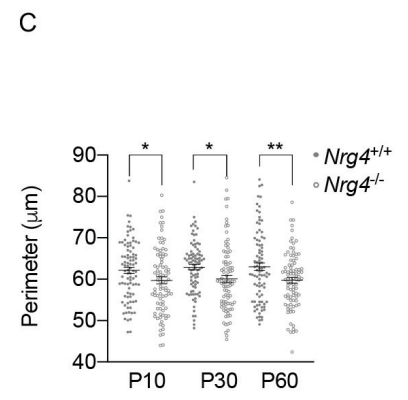
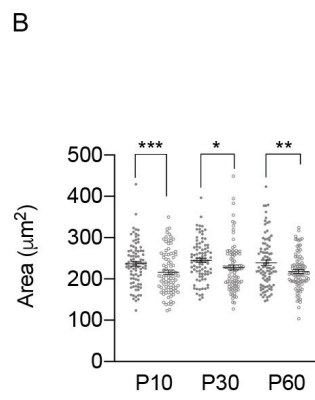
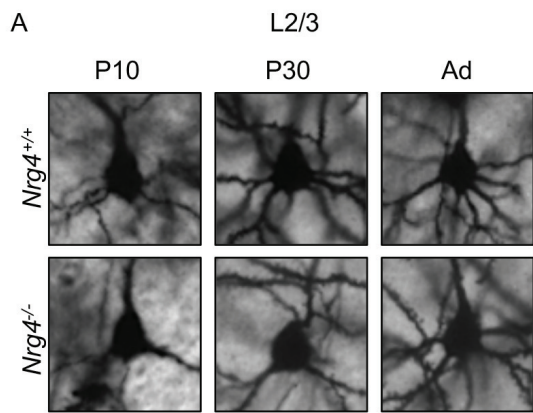
652 **Figure 6. The loss of NRG4 does not affect anxiety or response to novelty.** (A) Time
653 spent in the open arms of the elevated plus maze (EPM) was no different among P60 *Nrg4*^{+/+}
654 and *Nrg4*^{-/-} mice. (B) Total distance travelled and time spent in the centre (C) of the open-
655 field was similar between *Nrg4*^{+/+} and *Nrg4*^{-/-} mice. (D) P60 *Nrg4*^{-/-} mice spent a similar
656 amount of time exploring a familiar object and a novel object. (E) The object discrimination
657 percentage was similar between genotypes (calculated as the total amount of time spent
658 exploring the novel object divided by the total time spent exploring multiple by 100).

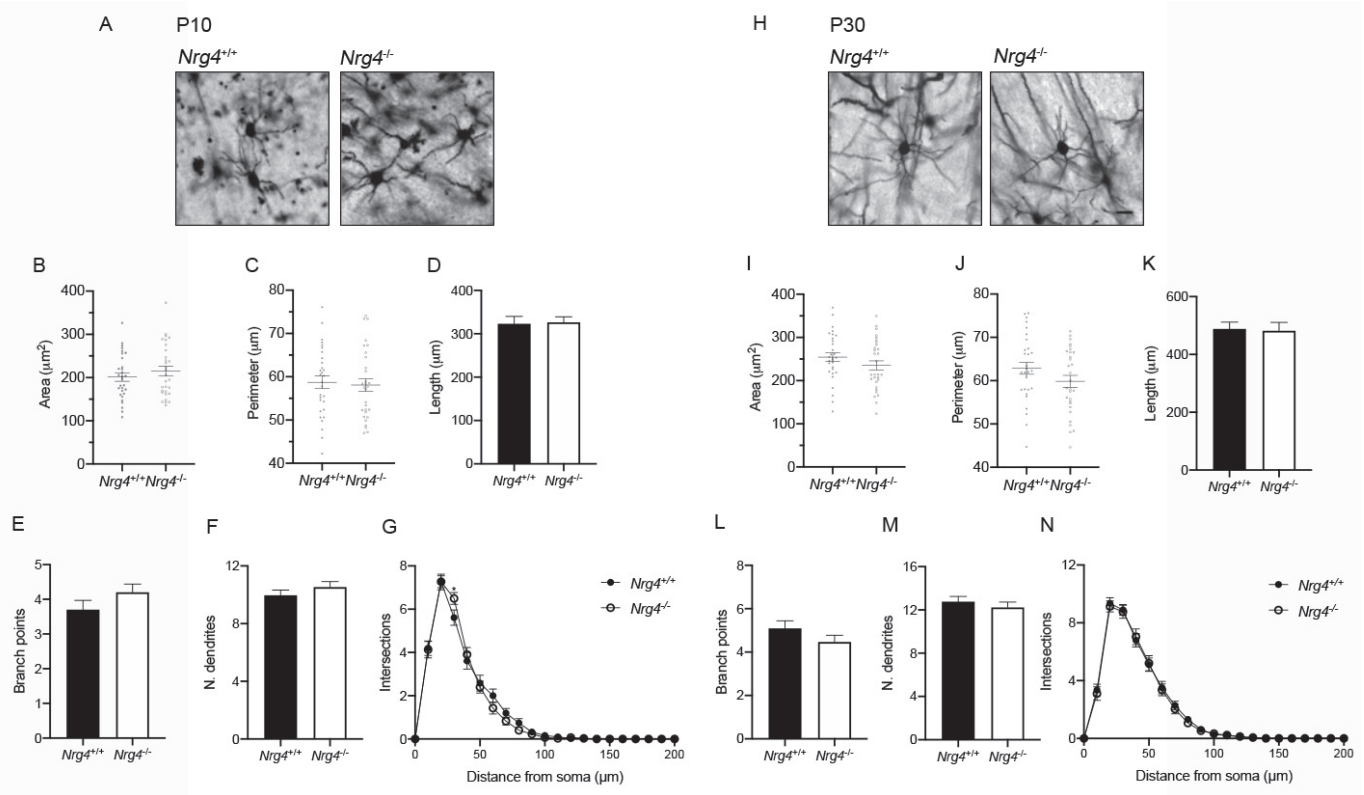
659

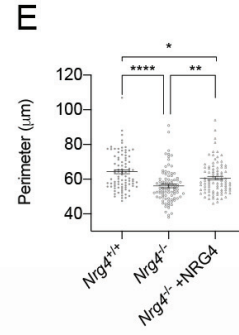
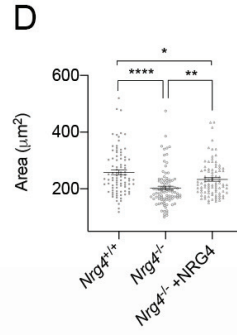
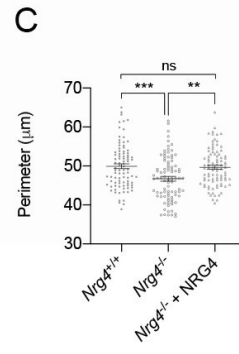
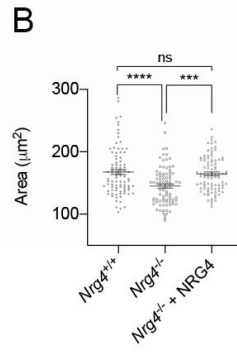
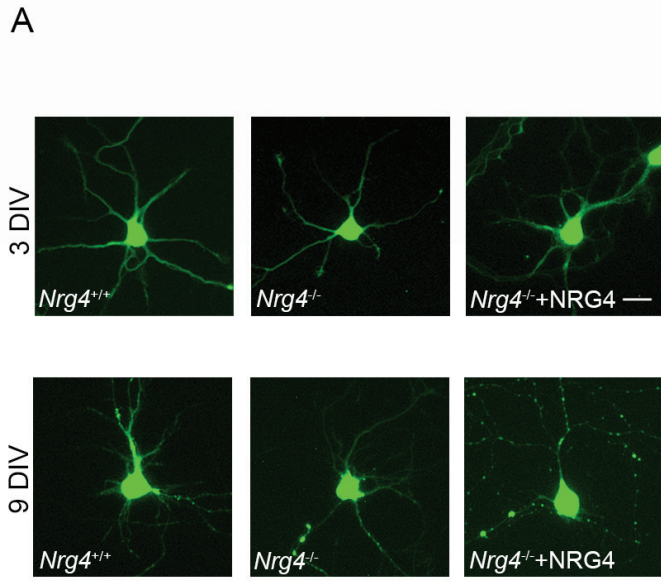
660 **Figure 7. NRG4 and ErbB4 co-expression with Ctip2, a major FEZF2 effector, in the**
661 **motor cortex of young postnatal brain.** (A-B) CTIP2 and FEZF2 (C-D) CTIP2 and NRG4,
662 and (E-F) CTIP2 and ERBB4 co-labelling in neurons from the motor cortex at postnatal day
663 10. Scale bar = 50 μm.

664

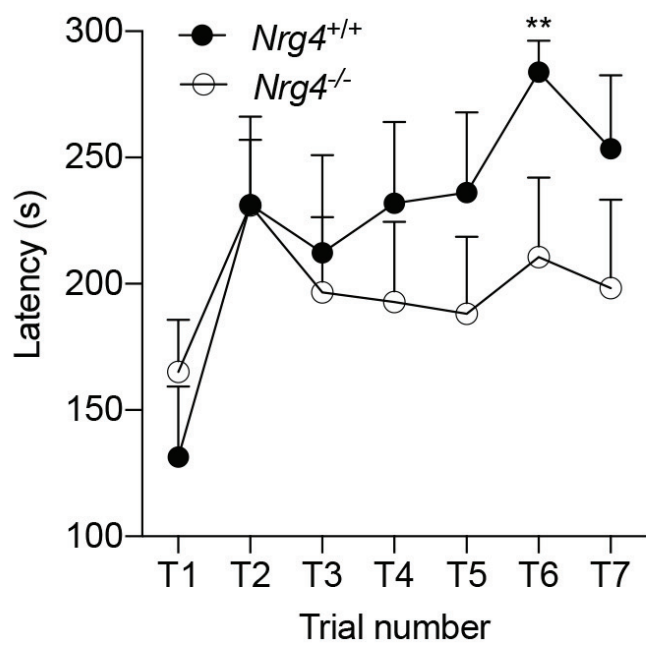




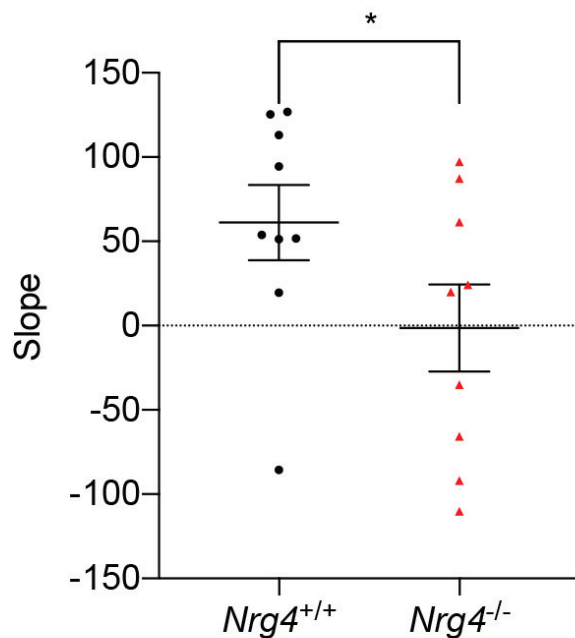




A



B



C

